Molecular Recognition and Self-Organization in Fluorinated Hydrocarbons

Frank H. Stillinger* and Zelda Wasserman

Bell Laboratories, Murray Hill, New Jersey 07974 *(Received November 16, 1977)*

Publication costs assisted by Bell Laboratories

Saturated fused-ring hydrocarbons offer a medium in which information can be stored at the molecular level. Selective fluorination encodes that information as a permanent binary pattern, which has characteristic geometric and electrostatic properties. Calculations have been carried out, specifically for fluorinated perhydrocoronenes, that suggest conjugate patterns on neighboring molecules can "recognize" each other and engage in a discriminating attractive interaction. Strategic selection of patterns permits control over the way in which these partially fluorinated hydrocarbons aggregate. Several possible applications are suggested for this type of directed formation of aggregation structures, including microtubule and membrane production, and a rudimentary type of molecular replication.

I. Introduction

One of the dominant themes uncovered by the recent advance of molecular biology has been the importance to life processes of specific molecular interactions. This theme is probably illustrated most strikingly in the complementary base pairing in DNA, which serves as a molecular medium for the storage, retrieval, and replication of hereditary information.[1] Specific interactions obviously are present as well in the remarkable discrimination that each variety of t-RNA exercises in binding only to its own amino acid.[2] Further examples of discriminating molecular interactions can be drawn from the phenomena of enzyme–substrate binding,[3] neural transmitter and opiate reception at synapses,[4] cell organelle self-assembly,[5] and pheromone-mediated chemical communication.[6]

For each of these examples it is believed that existence of the requisite "molecular recognition" hinges crucially upon details of chemical structure in the participating units. Those details surely include spatial arrangement and size of atoms, as well as electrostatic implications of charge density distribution and group polarizability. No doubt more subtle effects can be involved as well, such as hydrophobic interactions.[7] Indeed one of the most exciting current challenges to theoretical chemistry is the need for quantitative explanation of specific molecular interactions in biology.

Although the present work has its conceptual roots in molecular biology, its short-range objectives lie outside that discipline. An effort was made to identify novel nonbiological materials which could manifest discriminating molecular interactions. We propose that a family of saturated fused-ring hydrocarbons, specified in section II, can achieve this objective with carefully selected partial fluorination. The patterns of hydrogen and fluorine atoms borne by those molecules provide information storage, in binary form, at the molecular level. Conjugate patterns can "recognize" each other, and the resulting specific interactions thus present opportunities for controlled micromanipulation of the molecules involved.

We feel that the frankly speculative ideas and calculations reported in this paper deserve attention for several reasons. First, the suggested phenomena are novel, diverse, and potentially useful. Second, this is a general area of chemical research in which indiscriminate experimentation would be unlikely to succeed. Consequently a theoretical sifting of possibilities should precede serious laboratory

0022-3654/78/2082-0929$01.00/0

activity. Third, eventual laboratory demonstration of the phenomena suggested here could provide illuminating model molecular systems for specific interactions and modes of aggregation in molecular biology. In a sense this would bring the project full-circle to its conceptural origin, and repay the intellectual debt initially incurred.

Following discussion of the relevant hydrocarbon family (section II), we examine the chemical and structural effects of fluorination in section III. This is followed in section IV by advocacy of a simple method for estimating interaction energies between the fluorinated hydrocarbons, with specific application to substituted perhydrocoronenes. Section V discusses binary association constants, in vacuo and in various solvents, and estimates solvent pressure effects. Sections VI, VII, and VIII show how the information carried by the binary hydrogen–fluorine patterns transcribes directly and explicitly into various forms of aggregation, including linear polymers, membranes, and microtubules. The opportunity for molecular replication also emerges in this context, and our view of how it can be achieved is stated in section VIII.

For the most part we have felt obliged to leave detailed considerations of materials synthesis aside for the present exposition. Instead we have stressed the implications of accepted principles of structural chemistry, presuming simply that the molecules of interest could eventually be provided. In any event, we suspect that the rich opportunities uncovered here might stimulate exactly that type of creative synthetic chemistry required to produce the molecules discussed.

II. Saturated Hydrocarbon Family

The hydrocarbon family to be considered comprises an infinite number of members, the simplest of which is cyclohexane. All other members of the family consist of side-sharing cyclohexane rings, subject to the proviso that these puckered rings are always parallel translates of one another (i.e., they possess identical spatial configurations and orientations). Thus *trans*-decalin (two parallel side-sharing rings) is included, while *cis*-decalin is not. Some of the simpler members of this saturated hydrocarbon family are illustrated in Figure 1.

Although the minimum-energy configuration for cyclohexane is the "chair" form appearing in Figure 1, the molecule is quite flexible. At room temperature there are relatively rapid interconversions between equivalent (but distinct) "chair" forms, with an activation barrier estimated to be 10.5 kcal/mol. Under proper circumstances cyclohexane can also adopt a "boat" form, though this lies about 5 kcal/mol above the "chair" form energy.[8]

Side-sharing cyclohexane rings cannot display this flexibility. Bond length and angle requirements are not consistent with the deformations necessary to invert molecules at one or more carbon centers. These deformations could only be carried out by breaking covalent bonds, or at least severely violating the natural tetrahedral bonding directions at those carbon centers. Therefore we can regard all members of the hydrocarbon family, excepting cyclohexane, as essentially rigid frameworks.

This molecular rigidity has fundamental importance in the present investigation. It implies a permanent partitioning of hydrogen atoms between axial C–H bonds that remain perpendicular to the common midplane of the hexagons, and equatorial C–H bonds that radiate obliquely from the molecular periphery (see Figure 1). The rigid axial arrays of C–H bonds will serve as the binary information bearing medium in the subsequent analysis.

Letting n and b represent respectively the numbers of carbon atoms and of C–C bonds, it is easy to establish that

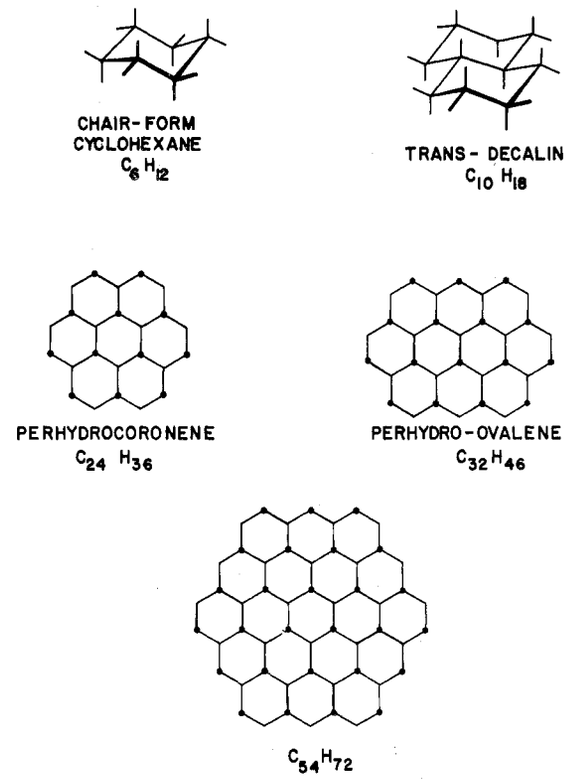

Figure 1. Family of saturated, fused-ring hydrocarbons. The first two examples are shown in perspective; the last three are represented schematically with upward axial C–H bonds as dark circles.

all of our saturated hydrocarbons conform to the general formula C_nH_{4n-2b}. The number of axial C–H bonds is always n (one at each carbon), and the number of equatorial C–H bonds is $3n - 2b$. The integers n and b can separately be either odd or even.

Although minor variations can be expected, it will be sufficiently accurate for present purposes to suppose that all bond angles in the rigid hydrocarbons have the common ideal value for tetrahedral bonding $\cos^{-1}(-1/3)$, or 109.47°. Furthermore we can assume that all C–C bonds have the same length 1.54 Å. Similarly all C–H bonds (whether axial or equatorial) should have lengths clustering closely around 1.1 Å.

III. Effects of Axial Fluorination

Substitution of fluorine for hydrogen in a C–H bond produces three principal effects that are important for the present study: (1) bond length increase; (2) increase in atomic size; (3) shift to substantially greater electronegativity. These are the changes which create opportunity for existence of specific interactions between partially fluorinated hydrocarbons.

With respect to (1), singly fluorinated carbons display C–F bond lengths around 1.4 Å. A trend toward slightly increasing length seems to exist as the carbon changes from primary, to secondary, to tertiary; the respective mean lengths are 1.39, 1.41, and 1.43 Å.[9] In all cases this represents an increment of about 0.30 Å over the corresponding C–H bond length. It should be kept in mind that carbon atoms in the saturated hydrocarbon family considered here are all secondary or tertiary.

van der Waals radii for H and for F atoms are listed by Pauling as 1.2 and 1.35 Å, respectively.[10] These radii illustrate effect (2) above, and reflect the larger number of electrons surrounding an F nucleus, compared to an H nucleus. On account of the Pauli exclusion principle, we expect pairs of nonbonded fluorine atoms to manifest repulsion at greater separation than would pairs of non-

bonded hydrogens; the quoted van der Waals radii are a quantitative verification of that expectation.

A pair of second-neighbor carbon atoms, both on the top or both on the bottom of one of the molecules discussed previously, will be separated by a distance equal to $(8/3)^{1/2}$ times the C–C bond length. This separation is 2.51 Å. Since twice the van der Waals radius for hydrogen (2.4 Å) is substantially less, no crowding between two hydrogen atoms as axial neighbors would arise.

In the case of two fluorine atoms, the corresponding van der Waals contact distance (2.7 Å) somewhat exceeds the nominal separation for axial neighbors. Nevertheless, the extra energy required to bring two nonbonded fluorine atoms to within the cited 2.51 Å is probably not very large. If that crowding energy were large, it would be hard to understand why C–F bond lengths *decrease* in the series of substituted methanes CH_3F, CH_2F_2, CHF_3, CF_4 while at the same time maintaining virtually undistorted tetrahedral bond angles.[9] Furthermore the crystal structure of polytetrafluoroethylene, $(-CF_2-)_n$, displays only a modest chain twist to relieve crowding.[11] Finally we note that it is in fact possible to fluorinate graphite to produce high molecular weight saturated perfluorocarbons with a characteristic fused hexagon structure.[12] Evidently there is no chemical difficulty in synthetically generating neighboring axial C–F bonds, and the rigidity of the carbon skeleton in our molecules should prevent substantial distortion away from the tetrahedral bond directions. In the remainder of this paper we shall regard each axial C–H bond as qualifying independently as a fluorination site.

It should be noted in passing that other halogens do not qualify for independent replacement of axial hydrogens, on account of their greater size. The van der Waals radius of Cl, for example, is 1.80 Å.[10] This is far too large to permit pairs of chlorine atoms to occupy adjacent axial positions. Thus we cannot expect to find a chlorocarbon analogue of the fluorocarbon phenomena under consideration.

With respect to point (3) above, it is appropriate to view fluorination in terms of a change in effective electrostatic charge on the axial atom. Several alternative methods are available to estimate H and F effective charges. Their implication is always the same, namely, that change from H to F is equivalent to a change from positive to negative net charge, in accord with the electronegativities of the elements, C, H, and F.[13]

It will be useful later to refer to the result of a specific calculation of the effective atomic charges q_H and q_F. For this purpose we can employ methane (CH_4) and methyl fluoride (CH_3F) as model compounds. Using measured geometries for these molecules and an appropriate value for the fluorocarbon dipole, along with the charge ratio inferred from Mulliken populations for Hartree–Fock wavefunctions,[14] one infers

$$q_H = 0.1041e_p$$
$$q_F = -0.2163e_p \qquad (3.1)$$

where e_p is the fundamental proton charge. We will assume that these charges are transferable, at least approximately, to the fluorinated hydrocarbons of primary interest in this study.

These considerations indicate that an arrangement of axial H and F atoms on the top or bottom surface of one of the rigid hydrocarbons constitutes a joint size and charge pattern. Both aspects will be important for the specific interactions between pairs of fluorinated molecules.

To illustrate the multiplicity of distinguishable patterns that are possible, we consider the specific case of perhydrocoronene, $C_{24}H_{36}$. By referring to Figure 1, one sees that the available set of 12 axial bonds on one side of the molecule has an arrangement with nominal threefold symmetry. Three of the positions form an inner triangle; the remaining nine are situated peripherally about that triangle. Figure 2 presents a few of the axial H, F patterns that could exist for perhydrocoronene. These patterns are paired with their "conjugates". Equivalent axial positions on conjugate patterns are located by reflection across a midline as shown in the figure; whenever H occurs in one of the pair, F occurs in the corresponding axial position of the other pattern, and vice versa. No pattern can serve as its own conjugate pattern (even permitting rotation), since the central triangle of three axial positions itself cannot satisfy such a criterion.

The number of distinct patterns for fluorination of the 12 axial positions on one surface of perhydrocoronene is impressively large. Table I provides an accounting, broken

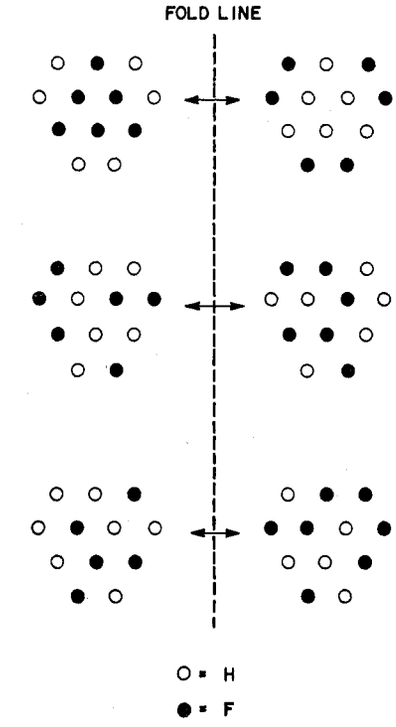

Figure 2. Conjugate pattern pairs for the 12 axial bonds on one surface of perhydrocoronene. Corresponding positions in the pairs are to be brought into contact by folding as indicated, to produce H, F contacts at each position.

TABLE I: Number of Distinct Axial Fluorination Patterns for One Surface of Perhydrocoronene[a]

No. of F's	No. of H's	Distinct patterns
0	12	1
1	11	4
2	10	22
3	9	76
4	8	165
5	7	264
6	6	312
7	5	264
8	4	165
9	3	76
10	2	22
11	1	4
12	0	1
	Total	1376

[a] We are indebted to Professors Cizek and Paldus (University of Waterloo) for correcting an error in the first version of this table.

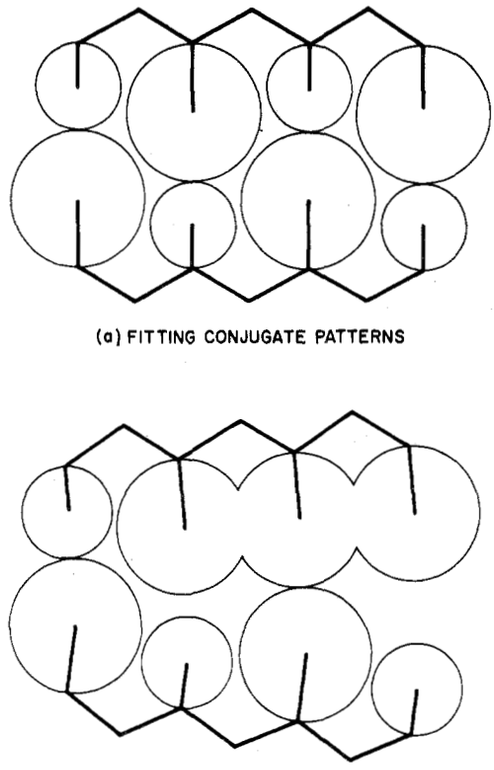

Figure 3. Effect of fluorine–fluorine mismatch. In (a) the conjugate patterns fit together with hydrogen–fluorine contacts (small and large circles, respectively) at each axial position. The unfavorable fluorine–fluorine contact in (b) forces other pairs apart due to molecular rigidity.

down by the numbers of H and F atoms involved. This enumeration does *not* count separately those patterns which differ only by rotation, however those differing by reflection *are* regarded as distinct. In all there are 1376 distinct patterns available for just one surface of perhydrocoronene. Considering both surfaces simultaneously, it is obvious that an enormous number of distinguishable isomers can exist for the molecule as a whole. It should also be obvious that numbers of patterns will be even larger for higher-molecular-weight members of the hydrocarbon family.

We propose that the desired specific interactions will be manifest between conjugate patterns. If two molecules bearing those conjugate patterns approach each other in such a way that corresponding axial bonds are aligned, electrostatically favorable, H, F contacts will occur simultaneously at each of the axial positions. In the case of two fluorinated perhydrocoronenes, this produces 12 simultaneous favorable charge pairs.

If an attempt is made to bring two nonconjugate patterns together, or a conjugate pair with a nonfitting relative orientation, repelling pairs of like-charged atoms would be forced together. Furthermore the greater atomic size and greater axial protrusion of two contacting axial fluorines should prevent close approach of other "correct" axial pairs, since the substrate molecules are quite rigid. These features are illustrated in Figure 3.

It is necessary to estimate quantitatively the strength of these interactions and their pattern specificity. Before constructing those estimates in the following section, it is proper first to ask if any known fluorocarbon phenomena support the proposed hydrogen–fluorine interactions, even in a rudimentary way. We suggest that at least four observations provide such support.

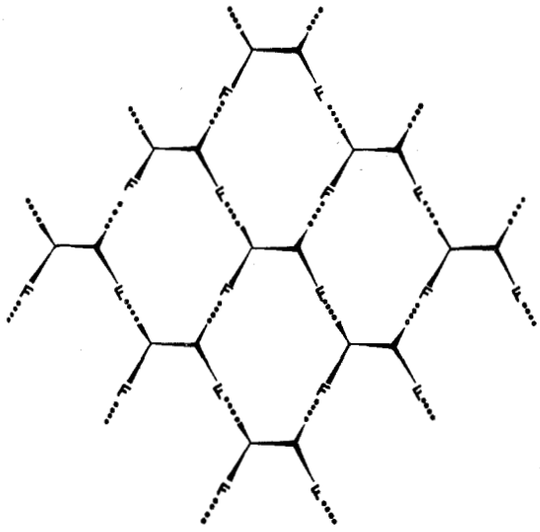

Figure 4. Possible network structure for 1,2-difluoroethane. All molecules have the same gauche form, with their dipole moments parallel. Each fluorine is in contact with a hydrogen on a neighboring molecule.

(a) An intramolecular hydrogen bond, with fluorine as proton acceptor, evidently can form in *o*-fluorophenol. Carlson et al. estimate this bond to have strength 1.44 kcal/mol,[15] by observing the relevant torsional frequencies.

(b) On the basis of NMR chemical shift measurements, Schneider has concluded that a weak but definite hydrogen bond forms between chloroform and 1-fluoropropane.[16] Again the fluorine atom acts as acceptor, now for a chloroform proton.

(c) Mixed crystals with 1:1 stoichiometry are known to form between hexafluorobenzene on the one hand, and benzene[17] or mesitylene[18] on the other hand. It has been argued[19] that large molecular multipole moments primarily produce the necessary "specific" interactions between unlike molecules, rather than an electron donor–acceptor complexation. These electrostatic interactions are analogous to those postulated for our own family of fluorinated hydrocarbons, and are powerful enough to be thermodynamically observed in the vapor phase.[20]

(d) 1,2-Difluoroethane exhibits classical symptoms of strong association that probably can best be explained in terms of preference for intermolecular H, F contacts. These symptoms include rather high boiling points for fluorocarbons of its molecular weight range ($T_b \approx 30$ °C, compared to −25 °C for 1,1-difluoroethane), and high liquid-phase dielectric constant ($\epsilon_0 \approx 34$ at 32 °C).[21] It is known that this substance has molecules which prefer the gauche form, with dipole moment 2.67 D.[22] Unlike the case with isomeric 1,1-difluoroethane, the structure of this molecule lends itself naturally to formation of extended structures with optimal H, F contact and with parallel molecular dipoles. One possibility is shown in Figure 4. It is obviously relevant to search for this, or similar, structures in the crystalline phase, but unfortunately those experiments have apparently not been undertaken.

IV. Interaction Calculations

Ideally, one would like to carry out potential energy calculations for pairs of fluorinated hydrocarbons, using ab initio methods of computational quantum mechanics. That is unfortunately not yet possible for molecules the size of those we have considered. Instead, it has been necessary to devise a semiempirical method for approximating the interactions of interest. However first we turn to a simple preliminary study of single axial contact for which an ab initio calculation can in fact be performed.

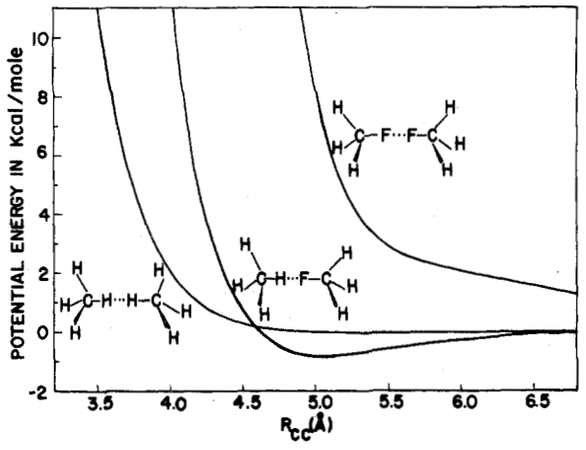

Figure 5. Hartree–Fock "4-31G" energies for axial contacts. In each of the three cases the contacting axial groups are exactly collinear, and the pendant methyl groups are eclipsed.

Thus we return temporarily to methane and methyl fluoride, and consider the three pairs of molecules H_3C–H···H–CH_3, H_3C–F···H–CH_3, and H_3C–F···F–CH_3. These pairs offer a reasonable model for collinear axial contacts between larger fluorinated hydrocarbons, provided the end methyl groups are rotated into an eclipsed arrangement.

We have carried out Hartree–Fock calculations for these pairs, in a Gaussian basis of atomic orbitals at the "4-31G" completeness level advocated by Pople.[23] Results are displayed in Figure 5 as separate potential curves for each of the three types of axial contacts, plotted against distance between carbon nuclei. Not only do these calculations show that the unlike-pair contact is energetically most stable (maximum binding 0.78 kcal/mol at R_{CC} = 5.06 Å), but they clearly reveal as well the atomic size and bond-length distinctions stressed earlier.

Two shortcomings of the Hartree–Fock approximation should be noted. First, it tends to overestimate molecular dipole moments; in the present case CH_3F is predicted to have moment 2.50 D, in contrast to the experimental value 1.85 D.[24] Second, dispersion attractions between molecules will always be absent in Hartree–Fock calculations. However we do not expect that removing these shortcomings would severely affect the results shown in Figure 5. In particular the relative vertical ordering of the curves should be preserved. Having made these observations, we conclude that the Hartree–Fock calculations support the basic qualitative concepts in our specific interaction proposal.

In order to describe the interactions of more complicated cases we have used an additive set of atom pair potentials $V_{\alpha\beta}(r)$, where species subscripts α and β represent C, H, or F. Consequently the total intermolecular potential for two molecules consists of a sum of such functions for all atom pairs comprising one atom in one molecule and the other atom in the other molecule. The specific form chosen for the $V_{\alpha\beta}$ is the following:

$$V_{\alpha\beta}(r) = A_{\alpha\beta} \exp(-b_{\alpha\beta}r) - C_{\alpha\beta}/r^6 + q_\alpha q_\beta/r \qquad (4.1)$$

The three terms are intended respectively to represent overlap repulsion between the atomic electron clouds, dispersion attraction, and Coulomb interaction between effective charges on the atoms. [Although each of the $V_{\alpha\beta}$ diverge to minus infinity as $r \to 0$, this unphysical behavior is manifest only in a small-r regime that is never used in our calculations.]

Effective charges q_H and q_F for hydrogen and fluorine, to be used in eq 4.1, have already been stated in eq 3.1.

TABLE II: Atom Pair Potential Parameters

Pair	$A_{\alpha\beta}$, kcal/mol	$b_{\alpha\beta}$, Å^{-1}	$C_{\alpha\beta}$, kcal Å^6/mol
FF	126200	4.60	118[a]
FC	162000	4.60	203[a]
CC	908000	4.59	363[a]
HH	9170	4.54	45.2[b]
HF	16900	4.57	62.7[b]
HC	0		0

[a] T. W. Bates, *Trans. Faraday Soc.*, 63, 1825 (1967). [b] R. A. Scott and H. A. Scheraga, *J. Chem. Phys.*, 42, 2209 (2965).

The effective charge q_C to be assigned to a given carbon will depend on the atoms bonded to it; we have assumed

$$q_C = -(\text{total attached H and F charge}) \qquad (4.2)$$

This choice preserves overall charge neutrality in each molecule by preserving it at each carbon atom.

The values used for parameters $A_{\alpha\beta}$, $b_{\alpha\beta}$, and $C_{\alpha\beta}$ are listed in Table II. We have adopted the values used by Bates, and by Scott and Scheraga, in their studies of molecular conformations. Although these authors did not find it necessary to incorporate effective atomic charges in their own atom pair potentials, it is our opinion that properties they examined were far less affected by these charges than the specific interactions at issue here. Also notice that the carbon–hydrogen function V_{CH} contains *only* the Coulombic term.

A general computer program was constructed to evaluate the interaction between two fluorinated perhydrocoronene molecules. In this case each molecule contains 60 atoms, so that 3600 atom-pair potentials have to be evaluated to give a net intermolecular interaction V. The separate molecules were treated as rigid bodies, with strict tetrahedral bonding at each carbon atom. Bond lengths used were 1.54, 1.12, and 1.43 Å for C–C, C–H, and C–F, respectively. All equatorial bonds remained unfluorinated during our calculations. In order to implement the interaction program, the operator must specify axial fluorination patterns on top and bottom of both molecules, and must select six configurational coordinates which determine relative position and orientation for the molecules. We found it convenient to use three Cartesian coordinates (x, y, z) for vector displacement between carbon-skeleton symmetry centers, and Euler angles (α, β, γ) for relative orientation, as shown in Figure 6.

Figure 7 presents results calculated for the total interaction energy V for a pair of identical fluorinated perhydrocoronene molecules. Each of these molecules bears the first pair of conjugate patterns shown earlier in Figure 2; one is on the top surface of the molecule and one is on the bottom surface. The curves shown represent the distance variation of V as the molecules approach each other in direct fashion; the molecular planes are parallel and their symmetry axes are collinear. On account of the threefold rotational symmetry of the molecules, there are six equivalent ways that the molecules can approach each other to bring conjugate patterns into proper contact. The curve labeling used in Figure 7 follows the convention established in Figure 2; namely, the patterns indicated approach each other in the manner obtained by folding across an imaginary vertical line between them.

One of the three curves in Figure 7 represents the "proper" approach for the conjugate patterns, bringing all 12 axial positions together with mutual contacts between unlike atoms. This curve obviously displays the lowest V, with a minimum value −18.1 kcal/mol achieved at separation 5.3 Å. The uppermost curve in Figure 7 brings

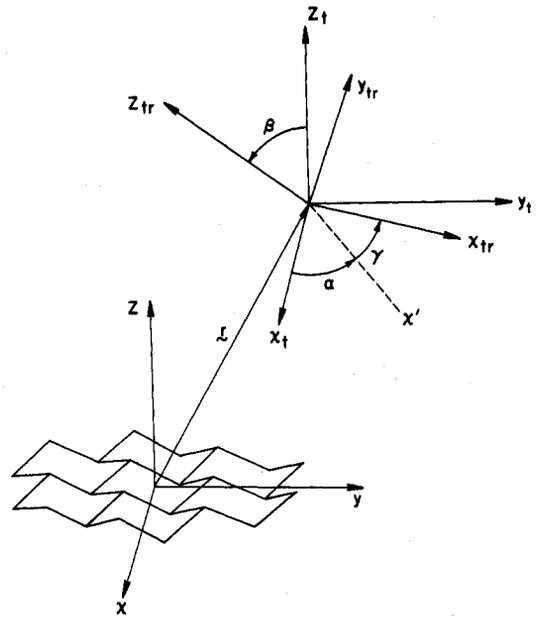

Figure 6. Orthogonal coordinates describing relative configuration of two molecules. After translation of the molecular center by $\mathbf{r} = (x, y, z)$, the body-fixed axes become x_t, y_t, z_t. This is followed by the sequence of Euler-angle rotations α(about z_t), β(about x'), γ(about z_{tr}). The body-fixed axes after translation and rotation are denoted by x_{tr}, y_{tr}, z_{tr}.

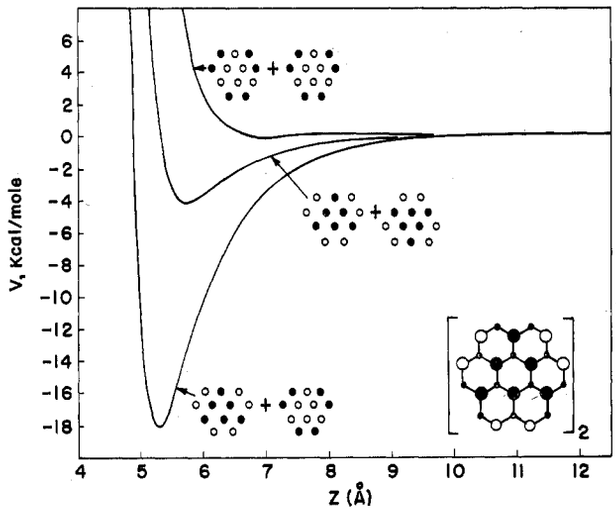

Figure 7. Dimer potential energy for the molecule schematically illustrated at the lower right. In that illustration the larger circles indicate upward-directed axial groups. Curve labeling follows the convention established in Figure 2; in all three cases the molecular midplanes are parallel and separated by z.

"wrong" atoms together at all 12 axial positions, and not surprisingly it indicates virtually no binding. The intermediate curve (minimum −4.2 kcal/mol at 5.7 Å) does not have axial bonds on the two molecules aligned, but interdigitating; the shallow minimum in this case can probably be attributed to the presence of some favorable diagonal contacts. These and other similar results for the given molecules lend quantitative credence to the presumption of pattern-specific interactions.

Figure 8 shows how V varies as the two molecules, initially in the deepest minimum of the preceding Figure 7, undergo a relative shear motion along the x direction. Obviously a very flat potential well exists for this type of deformation. However V begins to climb steeply beyond $\Delta x = \pm 0.4$ Å, at which stage the 12 favorable contacts all begin to be lost. A very similar result has also been found for y-direction shear.

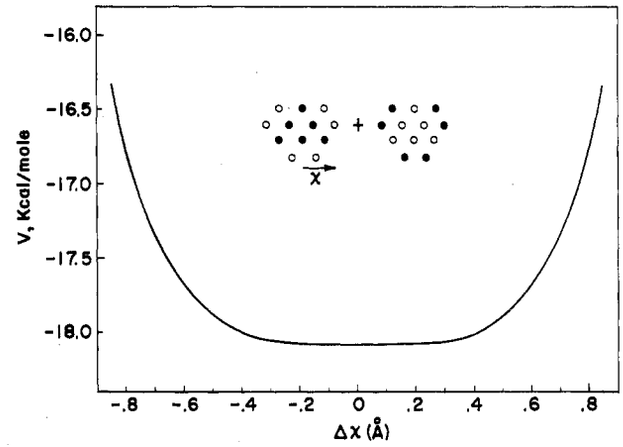

Figure 8. Side-slip dependence of potential for the dimer of Figure 7. $\Delta x = 0$ corresponds to the absolute minimum shown in Figure 7, with $z = 5.275$ Å and with corresponding axial groups collinear. The diagram indicates the direction of slip relative to the patterns.

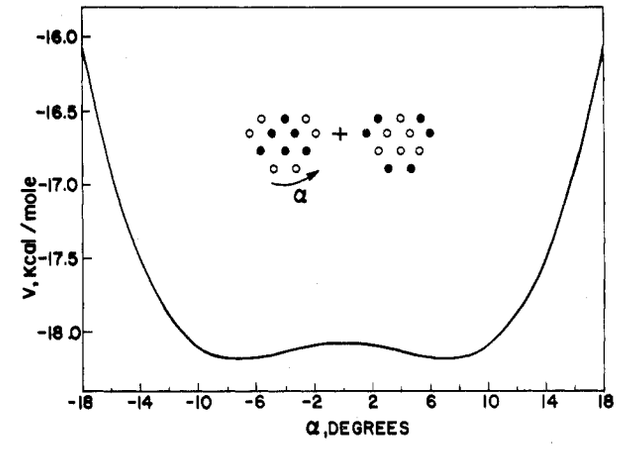

Figure 9. Dependence of dimer potential with respect to mutual rotation about the common perpendicular axis. The molecules are those shown in Figure 7, with separation $z = 5.275$ Å.

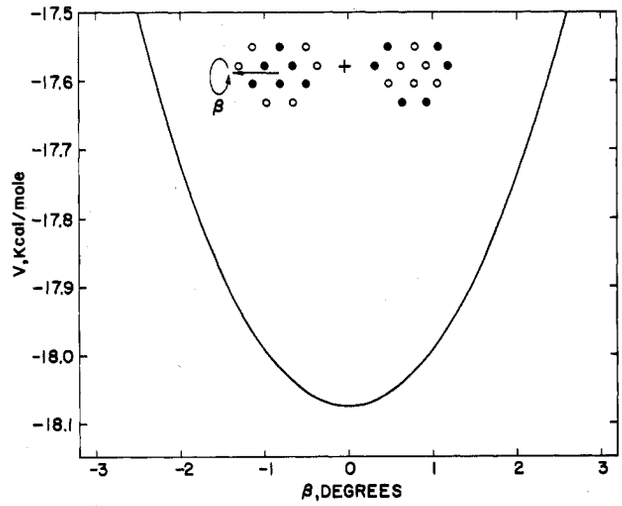

Figure 10. Tilt dependence of dimer potential for the molecules in Figure 7. The tilt axis resides in a molecular midplane; and the center–center distance is 5.275 Å.

The effect of rotation about the z axis (common molecular symmetry axis) is shown in Figure 9. This curve exhibits shallow minima at ±7° rotation, suggesting the possibility of small stable distortion from ideal axial-bond collinearity. However the extra stability indicated (0.10 kcal/mol) is very small, and would likely be strongly dependent upon precise values of potential parameters

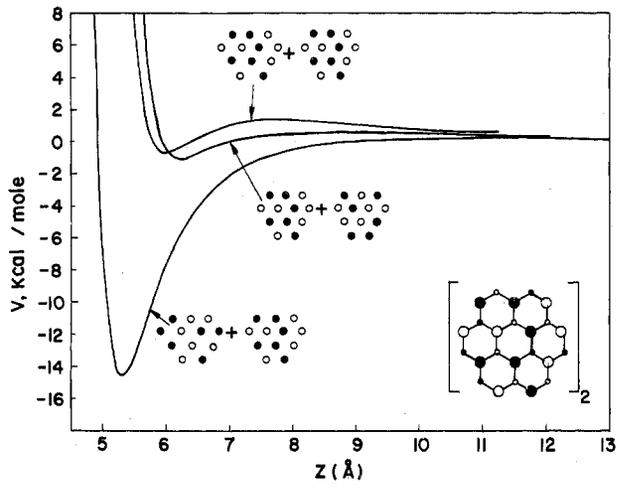

Figure 11. Dimer potential energy for the fluorinated perhydrocoronene illustrated at lower right. z is the distance between parallel molecular midplanes.

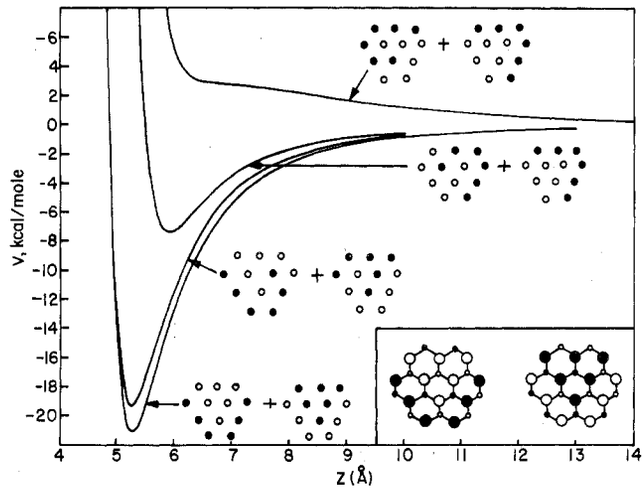

Figure 12. Pair potential curves for the molecules illustrated at the lower right. Molecular midplanes are parallel and separated by z.

(Table II). We regard this specific feature as uncertain. It seems safe to conclude that whatever the precise shape, it is nearly flat over the range $-12° \leq \alpha \leq +12°$.

The effect of rotating one molecule about the x axis (in the molecular plane) is provided by Figure 10. On account of the width of the molecule being rotated, this "tipping" clearly causes atom crowding for only a few degrees of rotation. The corresponding variation of V with respect to rotation about the y axis is nearly the same.

In order further to verify that these types of results extend to other patterns, we have also calculated V for two identical molecules each of which bear on top and bottom the second conjugate pair of patterns shown in Figure 2. Three curves are shown for this dimerization in Figure 11, with parallel molecular planes and collinear symmetry axes for the carbon skeletons. Just as in the analogous case presented in Figure 7, the properly positioned conjugate patterns clearly lead to the greatest stabilization (−14.6 kcal/mol at 5.3 Å). Shearing and rotational deformations away from this configuration of greatest stability lead to V variations similar to those of the preceding case. The existence of specific attraction between conjugate patterns seems not to depend in any major way upon the symmetry of those patterns.

Distance variation of V is shown in Figure 12 for a third example, again with collinear symmetry axes for the carbon skeletons. In this case the participating molecules are *not* identical. However each one contains patterns whose conjugates appear on the other. The two distinguishable geometries which bring conjugate patterns together correctly once again lead to considerably greater binding than otherwise. Specific interaction between conjugate patterns is manifested once again.

In each of the three molecular pairings examined, the axial patterns have all consisted of equal numbers (6) of H's and F's. We suspect that this is the situation for which the separate atom–atom interactions given in Table II are most reliable. If larger numbers of F's were crowded together within a pattern, it is possible that mutual repulsion of the resulting negative charges would tend to reduce the q_F below its value appropriate for less complete fluorination (see eq 3.1). We have simply avoided this possibility in our numerical studies.

V. Association Constants

As stressed in the Introduction, a primary goal of the present investigation is to establish connections between specific interactions and the modes of molecular aggregation. We are therefore obliged to calculate binding constants K_a for the reversible association reaction between two molecules M_1 and M_2 of the type discussed

$$M_1 + M_2 \rightleftarrows M_1M_2 \tag{5.1}$$

where as usual

$$K_a = [M_1M_2]/[M_1][M_2] \tag{5.2}$$

For this purpose we turn to the apparatus of statistical mechanics.

It is appropriate to continue to treat the fluorinated molecules M_1 and M_2 as rigid bodies, whose respective positions and orientations can be described by six-vectors $\mathbf{x}_1$ and $\mathbf{x}_2$ comprising center-of-mass positions and Euler angles (see Figure 6). The binding constant in vacuo ($K_a^{(0)}$) may be shown to have the following form (using classical statistical mechanics):

$$K_a^{(0)} = \frac{1}{16\pi^3}\int_D d\mathbf{x}_{12}\, \exp[-\beta V(\mathbf{x}_{12})] \tag{5.3}$$

Here V is the interaction potential for the pair, studied in the last section, and $\mathbf{x}_{12}$ is the six-vector describing *relative* position and orientation. As usual β represents $(k_BT)^{-1}$. The region of integration D is defined by the geometric convention according to which M_1 and M_2 are defined to form a bound dimer; certainly any reasonable definition would have configurations of maximum binding located within the interior of the six-dimensional region D.

The expression (5.3) for $K_a^{(0)}$ implicitly assumes that molecular vibrations are unaffected by the binding. Under some circumstances (such as the formation of hydrogen bonds to oxygen or nitrogen atoms) substantial frequency shifts can accompany binding, which would require inclusion in $K_a^{(0)}$ of the relevant vibrational partition functions. However for our fluorinated hydrocarbons no strong case seems to exist for such an effect, so we simply disregard it.

An accurate evaluation of $K_a^{(0)}$ would require evaluating V over a dense grid in D, followed by a suitable numerical evaluation of the integral in eq 5.3. However for present purposes we need only to make a crude estimate. Since the dominant contribution to the integral comes from a small region around the minimum of V, V_{min}, we can assume that the relevant region is determined by variations of the coordinates from their values at V_{min}, which cause

V to increase by amount k_BT. Within this effective binding region we assume that the integrand has the constant value $\exp(-\beta V_{sin})$.

For the sake of concreteness, we turn to the example illustrated earlier in Figures 7–10, and recall that this case displayed six equivalent ways of placing the conjugate patterns into proper contact. From the quantitative information gained earlier about that example, we conclude that the following coordinate variations are appropriate in estimating $K_a^{(0)}$ at 20 °C:

$$\begin{aligned} \Delta x_{12} = \Delta y_{12} &= 1.3 \text{ Å} \\ \Delta z_{12} &= 0.2 \text{ Å} \\ \Delta\alpha_{12} = \Delta\gamma_{12} &= 0.50 \text{ rad} \\ \Delta\beta_{12} &= 0.05 \text{ rad} \end{aligned} \tag{5.4}$$

Consequently we calculate

$$K_a^{(0)}(20\,^\circ\text{C}) \approx 6\left(\frac{1}{16\pi^3}\right) \exp(-\beta V_{min}) \times \Delta x_{12}\Delta y_{12}\Delta z_{12}\int_{-0.25}^{+0.25} d\alpha_{12} \int_0^{0.05} \sin\beta_{12}\, d\beta_{12} \times \int_{-0.25}^{+0.25} d\gamma_{12} = 1.3 \times 10^7 \text{ Å}^3 \tag{5.5}$$

This is the value appropriate for definition (5.2) expressed in terms of the concentration units molecules/Å^3; in the more familiar concentration units mole/liter the result (5.5) becomes

$$K_a^{(0)}(20\,^\circ\text{C}) \approx 7.8 \times 10^3 \text{ L/mol} \tag{5.6}$$

Needless to say, $K_a^{(0)}$ will increase as temperature declines.

A formal expression analogous to (5.3) is also available for association in a solvent. Of course this is the more relevant situation for real experiments that might be carried out on specific interactions. The only change is that interaction potential V must by replaced by the potential of mean force W:[25]

$$K_a = \frac{1}{16\pi^3}\int_D d\mathbf{x}_{12} \exp[-\beta W(\mathbf{x}_{12})] \tag{5.7}$$

Unlike V, W will generally depend on temperature, and it will reflect the individual properties of each solvent. Unfortunately no simple procedure is available to evaluate W for any given solvent, analogous to the atom-pair sum used in the preceding section for V. Probably the best tool for investigating W at present is computer simulation, still a massive undertaking.

Nevertheless we can make a few general observations about the effect of solvents on association equilibrium for our fluorinated hydrocarbons. It is reasonable that "good" solvents will have $K_a < K_a^{(0)}$, while "poor" solvents will have $K_a > K_a^{(0)}$. This stems from the obvious fact that a dissociated pair $M_1 + M_2$ exposes more net surface to solvent than does the dimer M_1M_2. "Good" solvents effectively encourage that greater exposure and shift the equilibrium toward dissociation; "poor" solvents do just the reverse and thus enhance binding. We suspect that methanol and ethylene glycol will prove to be "poor" solvents for the fluorinated hydrocarbons under discussion, and hence may be media of choice to study enhanced binding.

Just as variation in solvents induces change in W and in K_a, so too can variation in external pressure p cause analogous change in these quantities. For solute molecules at least as large as the substituted coronenes the effect should indeed be substantial. One way of expressing the expected trend is to say that increased pressure tends to make solvents poorer; an equivalent statement is that the association process is accompanied by a negative volume change. In any case the experimenter can increase K_a by increasing p.

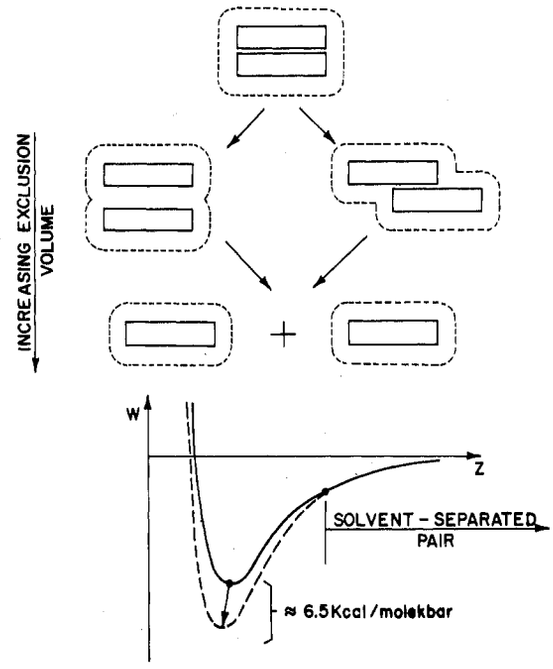

Figure 13. Effect of increased pressure on dimer association. The fluorinated hydrocarbons are shown edge-on in simplified fashion merely as rectangles. The dotted curves surrounding them represent exclusion envelopes, within which the centers of solvent molecules are sterically prevented from penetrating.

Figure 13 schematically shows what is at the heart of the pressure effect on association. The net volume excluded to solvent molecules by the solute particles is larger when they are apart than when they are bound together. Since free volume is a particularly precious commodity at high pressure, there develops a driving force to minimize volume excluded to solvents by solutes. In other words, binding increases.

For solvent molecules 5 Å in diameter, we estimate (from the crystal structure of perhydrocoronene[26]) that the solute binding entails an exclusion volume reduction Δv of about 450 Å^3. This implies that the binding-region value of W will approximately incorporate a term $-p\Delta v$, which increases binding strength by 6.5 kcal/mol kbar. If our earlier method of estimating $K_a^{(0)}$ is still valid for this hypothetical solvent, we expect for the molecules in Figures 7–10 that

$$K_a(20\,^\circ\text{C}, 1 \text{ kbar}) \approx 5.3 \times 10^8 \text{ L/mol} \tag{5.8}$$

a marked increase, indeed.

In truth, this pressure effect will also operate for "incorrect" contacts between the solute molecules. However these contacts do not allow the solutes to fit together very well, so the corresponding Δv's are smaller than for the "correct" fit between conjugate patterns. Thus increased pressure in a solvent should increase the specificity of interaction.

In closing this section it may be worth reminding the reader of an obvious fact. For pattern-bearing molecules larger than the fluorinated perhydrocoronenes, the binding constants for pairs bearing conjugate patterns will surely be substantially greater. In the large-molecule limit, binding energies and ln K_a values would become proportional essentially to molecular surface area.

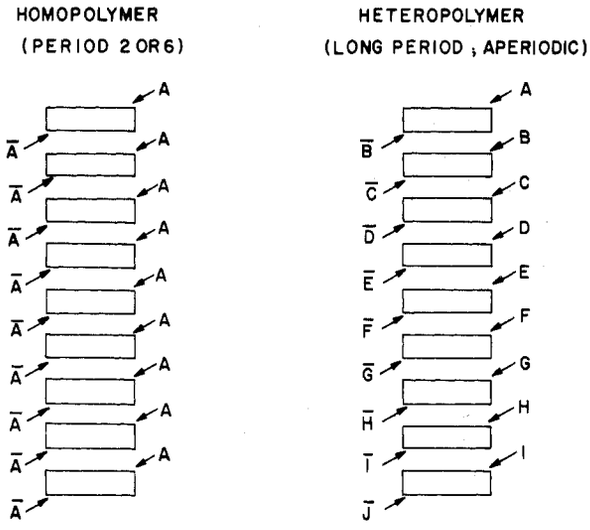

Figure 14. Formation of linear aggreates. The fluorinated hydrocarbons in side view again are caricatured simply as rectangles. The patterns are indicated by capital letters; $\bar{A}$ is the conjugate pattern for A, etc.

VI. Directed Polymerization

In the case of molecules bearing conjugate patterns on top and bottom surfaces, the association process need not stop with formation of dimers, of course. Free surfaces on dimers can add a third molecule, etc., to form eventually long linear homopolymers if the prevailing conditions permit. Examination of models shows that these homopolymers will have monomer units in identical configurations every second or every sixth position, depending on the symmetries of the patterns carried. These distinct periodicities should be manifest in x-ray diffraction patterns for the polymeric material.

Results displayed in Figures 7, 11, and 12 show that the specific interactions that develop between conjugate patterns are relatively short ranged. Consequently the association constants for successive stages of formation of a linear polymer ought to be nearly independent, and nearly equal to those for the dimerization stage.

Since extensive polymerization will produce rodlike aggregates, and since rigid rods at sufficiently high concentration undergo an isotropic–nematic phase transition,[27] it is possible that association of the type discussed can produce liquid-crystal phases.

A collection of fluorinated molecules, no one species of which is capable of homopolymerization, might nevertheless form a heteropolymer. Assuming that the requisite pattern pairs are present somewhere in the starting mixture, the molecules should sort themselves out by normal Brownian motion, and then bind to the appropriate partners. The resulting linear aggregate may have a long periodicity, or may be aperiodic, depending on what monomers are supplied. The homopolymer and heteropolymer aggregates are symbolically indicated in Figure 14.

In the heteropolymer case shown in Figure 14 it is clear that the patterns placed on the participating monomers constitute a "recipe" or "blueprint" for the formation of that aggregate. This is a case wherein translation of the binary code into aggregation order and form is clear and explicit. Furthermore, the "blueprint" becomes the construction material, which strikes one as an efficient use of resources.

To the extent that control has been exercised over order in the heteropolymer through the binary hydrogen–fluorine code, a mechanism exists for bringing together chemically reactive groups in a preassigned linear sequence for synthetic purposes. Thus the fluorinated hydrocarbon units could act as "molecular tugboats" to position fragments temporarily attached to them at equatorial positions on the hydrocarbon skeleton.

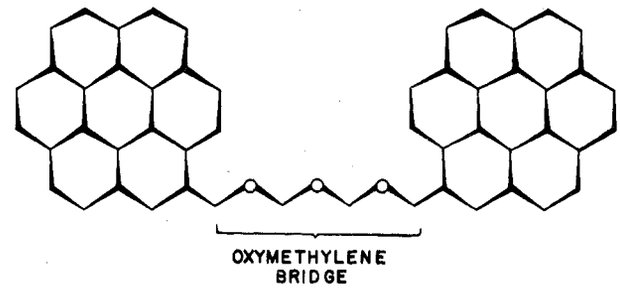

Figure 15. Pair of perhydrocoronene units linked by an eight-bond oxymethylene chain.

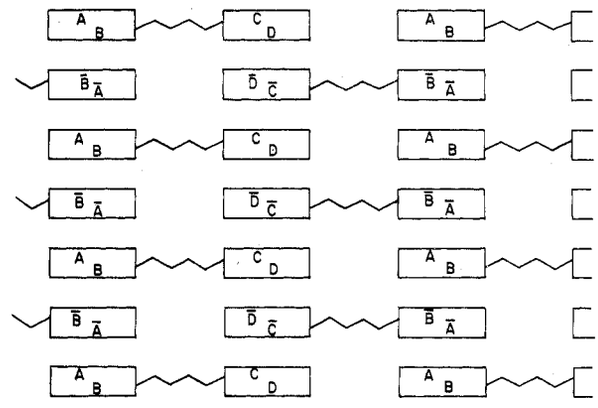

Figure 16. Two-dimensional sheet, or membrane, formed by aggregation of double units such as that shown in Figure 15. Two species of double units are employed, but if A, B, C, D are identical with $\bar{D}$, $\bar{C}$, $\bar{B}$, $\bar{A}$ respectively, the two species becomes identical.

VII. Extended Structures

One way to enlarge the possibilities for aggregation forms would be to link together pairs of fluorinated hydrocarbon units by a suitable covalent chain. The resulting double units then would possess four surfaces to carry the basic patterns. We shall see that proper selection and placement of patterns on the four surfaces can in principle lead to controlled production of several new types of extended structures. Once again the binary patterns constitute instructions for production of those structures.

Figure 15 shows two perhydrocoronene units joined by an eight-bond oxymethylene chain, with terminal attachments at equatorial positions. This bridge entails no steric repulsions with nearby equatorial hydrogens on the perhydrocoronene units that would force distortions from the planar zigzag configuration shown in Figure 15. Although relatively free rotations about the oxygen atoms in the chain are possible, there are synthetic techniques available for inhibiting such rotations if necessary; these include replacement of the central O by CH_2, incorporation of bulky side groups, and use of two parallel chains to form a macrocyclic connection between the pattern-bearing units.

One of the most interesting opportunities offered by two-unit linkage is the ability to cause membrane formation, that is, aggregates in the form of two-dimensional sheets. In its simplest version, this requires selection of patterns that stack as shown in Figure 16. While considering this mode of directed aggregation, it must be kept in mind that the patterns involved have to possess the proper orientations relative to the covalent chains, for otherwise an extended two-dimensional structure will fail

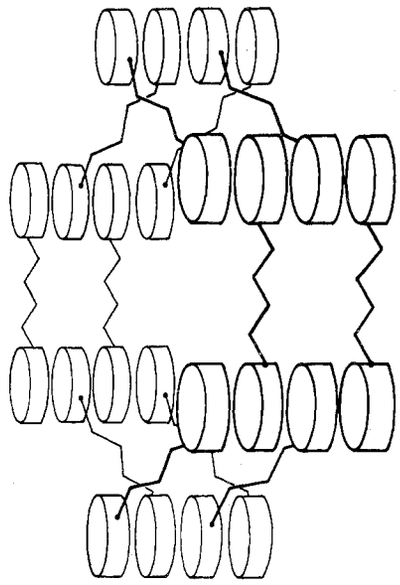

Figure 17. Aggregation of double units to form a microtubule. The pattern-bearing units (shown here simply as short cylinders) are stacked in six columns which are linked laterally by the covalent bridges.

to grow. The case illustrated in Figure 16 involves two different types of double units incorporating eight patterns; however it is also possible to arrange for membrane formation with just a single species of double unit.

The scientific importance of this membrane formation procedure lies in the ability to "engineer" the structure at will, and in particular to control the size and chemical nature of pores in the membrane. It is obvious that one degree of control lies in the choice of length and chemical structure of the connecting covalent linkages. It is also possible to arrange for the necessary insertion of monomer units into the membrane by adroit choice of patterns, which in turn affects pore size. Variations in pore character naturally affect the osmotic transport properties of the membranes, and should allow considerable synthetic control over permeation selectivity.

One can select and place patterns on the double units to make the structure close on itself, instead of stretching outward to form a sheet. The result is a microtubule, shown in Figure 17. If such a tubule were formed by self-assembly in solution, it would be filled with solvent. However it subsequently should be possible to remove the low molecular weight solvent by evaporation to leave an empty tubule. The interior diameter of a tubule could be made to occur in the 50 Å range, constituting potentially the basis for manufacturing waveguides for short-wavelength radiation. Probably no competing technique exists for fabricating such narrow waveguides. These microtubules might also have application in design of active, but nonbiological, "nerve fibers".

Finally, options also exist for aggregation of double units into three-dimensional channeled arrays. These would constitute an hexagonal array of side-sharing microtubules. The covalent chains emanating laterally would connect to three neighboring columns, rather than two as shown in Figure 17. In some respects these microtubule arrays might have molecular sieve properties analogous to those of the naturally occurring zeolites, which likewise possess channels.[28]

VIII. Intercalation and Molecular Replication

We have noted earlier that the natural separation between successive units bound together with contacting conjugate patterns is about 5.3 Å. Hence if two pattern-bearing units were to be held about 10.5–11.0 Å apart in parallel configuration they would form a natural cleft into which a third unit could bind (presuming it possessed the proper conjugate patterns). Indeed the binding in such a cleft would be quite strong since two pairs of matched patterns are simultaneously involved. In terms of results adduced in section IV, a cleft binding energy of 30 kcal/mol would not be unexpected for fluorinated perhydrocoronene units.

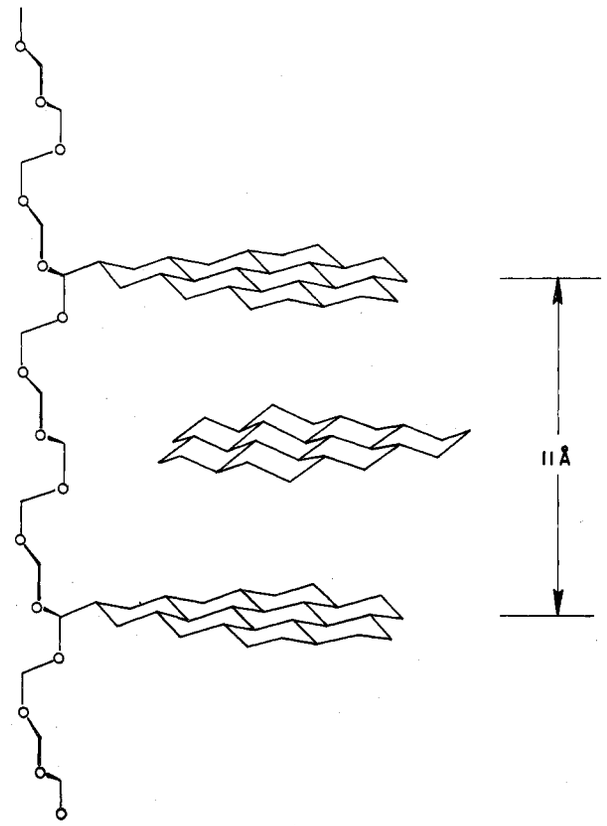

Figure 18. Intercalation of a pattern-bearing unit in a cleft formed by two chain-bound units.

A specific means for achieving a cleft arrangement is indicated in Figure 18. The seven-ring perhydrocoronene skeleton has been augmented by an eighth ring, which becomes a convenient point of attachment to an oxymethylene chain. Twelve bonds along the chain separate the attached pair, and when the chain has the extended spiral conformation shown, the units will be about 11 Å apart (according to models we have built). As discussed earlier, the rotational freedom within the oxymethylene chain can be quenched somewhat by chemical modification. In any case some freedom for motion of the bound units is probably desirable to facilitate the intercalation of a unit from the ambient solution.

These cleft-forming structures would constitute a powerful separation device for a solution containing monomeric units with a random collection of patterns. The clefts would preferentially bind monomers with the correct pair of conjugate patterns which (after removal of the ambient random mixture) could be stripped away in pure form by appropriate change in temperature, pressure, solvent, etc. Having in hand such an effective separation technique would permit the technology of pattern creation and utilization to "bootstrap" to a level of greater control over molecular aggregation. In the long run, one also cannot overlook the possibility that these clefts might constitute catalytic sites for synthesis of desired patterns.

This intercalation structure may also hold the key to a form of molecular replication. A sequence of patterned

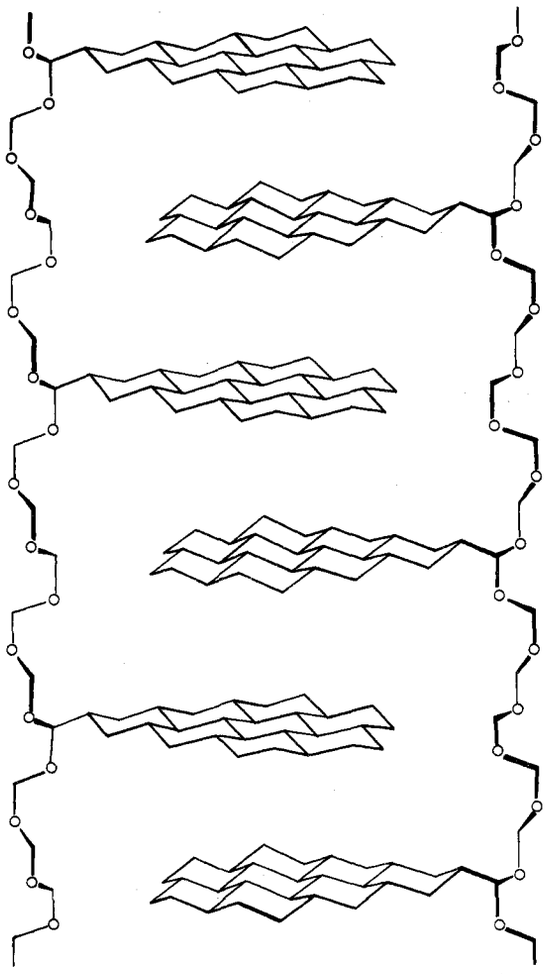

Figure 19. Complementary strands of pattern-bearing units.

units located every twelfth bond along an extended oxymethylene chain will present a sequence of clefts that could all be filled with the proper monomers, and then those monomers could themselves be chemically linked by another oxymethylene chain. The result, indicated in Figure 19, is a sequence of units (and clefts) complementary to the starting structure. If these complementary strands were then peeled apart, the new strand could in principle serve as template for formation of a replica of the old strand.

This replication process is analogous to that which occurs biochemically with DNA. However complementarity has a different meaning in the present case, in that neighboring *pairs* of units on one strand contribute to selection of a single unit for the new strand. In contrast, the bases in DNA exhibit one-on-one selection (guanine with cytosine, adenine with thymine). In order to avoid the possibility of information degradation at free ends of successive generations of replicating strands, it would be desirable to have the structures illustrated in Figure 19 each the parts of closed loops with no free ends. The resulting cyclic macromolecules would constitute fluorinated hydrocarbon analogues of the cyclic bacterial plasmids that have recently played such a prominent role in recombinant DNA research. Synthesis and study of the present nonbiological analogues would however completely avoid the dangers alledgedly posed by that type of biochemical research.[29]

IX. Conclusion

An obvious conclusion to draw from the present theoretical study is that synthetic techniques need to be developed to produce pure samples of the fluorinated hydrocarbons mentioned above. This would permit observation of the specific interaction postulated. Having in hand those substances would also permit electron diffraction and crystallographic studies to confirm or deny our assumptions about bond lengths and angles. It would also be illuminating to have measurements of dipole moments for selected members of our molecular family to check on the charge assignments stated earlier in eq 3.1 and 4.2.

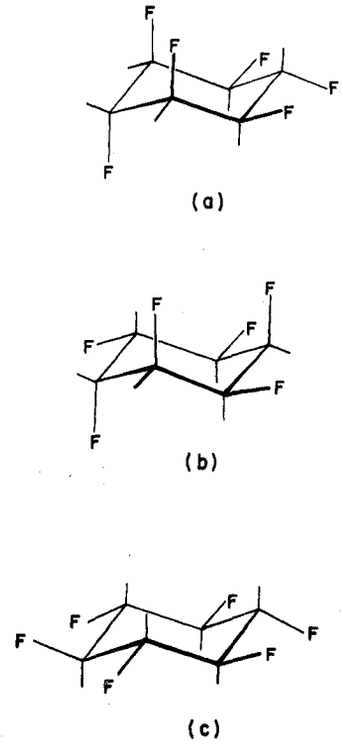

Figure 20. Three distinct isomers of hexafluorocyclohexane. Cases (a) and (b) can engage in self-aggregation through axial pattern contacts; (c) cannot.

There are some cases of partially fluorinated cyclohexane whose synthesis would probably not be inordinately difficult on the one hand, and whose physical properties would likely manifest the specific attractions discussed. Figure 20 shows three distinct hexafluorocyclohexanes that are relevant. Cases (a) and (b) could separately aggregate as indicated earlier in Figure 14. Since these are polar molecules the linear aggregates would have a large dipole moment. Case (c) presumably would have little or no such aggregation tendency. Although (a) and (b) can invert from one chair form to another, they are self-equivalent under this transformation. Fluorine repulsions should maintain (c) in the equatorial conformation shown.

It is at least as important to push ahead with theoretical studies. Quantum mechanical calculations are certainly feasible (at the Hartree–Fock level) for the interaction potential surfaces for several pairs of small fluorinated hydrocarbons. The pair potentials for 1,2-difluoroethane and for 2-fluoropropane are good candidates to enrich knowledge in this area. The quantitative information gained could be valuable in revising parameters in Table II, or even in motivating a change to more accurate means of calculating large-molecule potentials than the atom-pair sum used in section IV.

Presuming that a reliable general scheme is eventually available for estimating interactions, computer simulation studies (both Monte Carlo and molecular dynamics) ought to be applied to examination of the modes of aggregation in liquid solvents.

We believe the prospects for many exciting advances in this general area easily warrant the expenditure of considerable effort, both experimental and theoretical.

References and Notes

(1) J. D. Watson and F. H. C. Crick, *Nature (London)*, **171**, 737, 964 (1953).
(2) D. H. Gauss, F. von der Haar, A. Maelicke, and F. Cramer, *Annu. Rev. Biochem.*, **40**, 1045 (1971).
(3) W. N. Lipscomb, *Chem. Soc. Rev.*, **1**, 319 (1972).
(4) C. B. Pert and S. H. Snyder, *Science*, **179**, 1011 (1973).
(5) W. Herzog and K. Weber, *Proc. Natl. Acad. Sci. U.S.A.*, **74**, 1860 (1977).
(6) D. Schneider, *Sci. Am.*, **231**, No. 1, 28 (1974).
(7) F. Franks, *Water, Compr. Treat.*, **4**, 1 (1975).
(8) F. A. Bovey, "Nuclear Magnetic Resonance Spectroscopy", Academic Press, New York, N.Y., 1969, pp 188–194.
(9) A. Yokozeki and S. H. Bauer, *Top. Curr. Chem.*, **53**, 71 (1975).
(10) L. Pauling, "The Nature of the Chemical Bond", 3rd ed, Cornell University Press, Ithaca N.Y., 1960, p 260.
(11) C. W. Bunn and E. R. Howells, *Nature (London)*, **174**, 549 (1954).
(12) D. T. Clark and J. Peeling, *J. Polym. Sci.: Chem.*, **14**, 2941 (1976).
(13) Reference 10, p 90.
(14) L. C. Snyder and H. Basch, "Molecular Wave Functions and Properties", Wiley, New York, N.Y., 1972.
(15) G. L. Carlson, W. G. Fateley, A. S. Manocha, and F. F. Bentley, *J. Phys. Chem.*, **76**, 1553 (1972).
(16) W. G. Schneider in "Hydrogen Bonding", D. Hădzi and H. W. Thompson, Ed., Pergamon Press, New York, N. Y., 1959, p 55.
(17) C. R. Patrick and G. S. Prosser, *Nature (London)*, **187**, 1021 (1960).
(18) T. Dahl, *Acta Chem. Scand.*, **25**, 1031 (1971).
(19) C. L. Watkins and W. S. Brey, Jr., *J. Phys. Chem.*, **74**, 235 (1970).
(20) E. M. Dantzler and C. M. Knobler, *J. Phys. Chem.*, **73**, 1602 (1969).
(21) R. J. Abraham and R. H. Kemp, *J. Chem. Soc. B*, 1240 (1971).
(22) S. S. Butcher, R. A. Cohen, and T. C. Rounds, *J. Chem. Phys.*, **54**, 4123 (1971).
(23) R. Ditchfield, W. J. Hehre, and J. A. Pople, *J. Chem. Phys.*, **54**, 724 (1971).
(24) R. D. Nelson, Jr., D. R. Lide, Jr., and A. A. Maryott, *Natl. Stand. Ref. Data Ser., Natl. Bur. Stand.*, **No. 10** (1967).
(25) T. L. Hill, "Statistical Mechanics", McGraw-Hill, New York, N.Y., 1956, Section 40.
(26) F. Halla and W. R. Ruston, *Acta Crystallogr.*, **4**, 76 (1951).
(27) L. Onsager, *Phys. Rev.*, **62**, 558 (1942); *Ann. N.Y. Acad. Sci.*, **51**, 627 (1949).
(28) W. M. Meier and J. B. Uytterhoeven, *Adv. Chem. Ser.*, **No. 121** (1973).
(29) L. F. Cavalieri, *N.Y. Times Mag.*, **126**, 8 (Aug 22, 1976).

Conformational Analysis of Substituted Alkenes by Low Resolution Microwave Spectroscopy

Wayne E. Steinmetz,* John Hollenberg,[1] Fred Hickernell,[1] Carl E. Orr,[1]

Seaver Chemistry Laboratory, Pomona College, Claremont, California 91711

and LeRoy H. Scharpen

Surface Science Laboratories, 4151 Middlefield Road, Palo Alto, California 94304

(Received August 4, 1977; Revised Manuscript Received February 6, 1978)

Publication costs assisted by Pomona College and the Petroleum Research Fund

The low resolution microwave spectra of 5-hexenyl 1-formate and a series of 1-haloalkenes and trifluoroacetates of primary olefinic alcohols were examined. In most cases, only one conformer was observed. The evidence is consistent with the claim that the carbon–carbon double bond assumes a skew orientation to the side chain. Both s-trans and gauche conformations of the carbon side chain were found. The low resolution data provide only a single check and some of the proposed conformations, particularly those of the esters, must be regarded as tentative.

Introduction

Detailed gas phase conformational analyses of alkenes have been limited largely to derivatives of propene.[2-6] All these studies demonstrate the existence of the so-called skew conformer in which the side chain is oriented at ca. 120° to the plane of the double bond ($\chi_1 \sim 120°$, Figure 1a). This generalization is consistent with qualitative infrared studies of alkenes.[7,8] This low resolution microwave study was begun to test whether the skew conformation is characteristic of olefins. A combination of this parameter and the general features of alkane conformations[9] would permit the prediction of the conformation of important natural products such as insect pheromones and lipids. Low resolution microwave spectroscopy (LRMW) has been shown to be a rapid tool for semiquantitative, gas phase conformational analysis.[9-11] In this technique each near-prolate, polar conformer gives a symmetric top spectrum (Figure 2) which yields rotational constants and crude relative intensities.

Experimental Section

The 1-halo-2-propenes and *trans*-1-halo-2-butenes were obtained from commercial sources and were purified when necessary by gas phase chromatography. The other bromoalkenes were prepared by a two-step procedure.[12] The corresponding alcohol (Chemical Samples Co.) was tosylated with tosyl chloride in dry pyridine at 0 °C and the tosylate was allowed to react with anhydrous potassium bromide in dimethylformamide at 130–160 °C. In an attempted synthesis of 1-fluoro-5-hexene, 5-hexenyl 1-formate was obtained as a product of the side reaction of the tosylate with the solvent. Trifluoroacetate esters were obtained by allowing the alcohol to react with a slight excess of trifluoroacetic anhydride in ether. Some alcohols were commercially available and the others were prepared by one of two procedures. All alcohols or their precursors were purchased from Chem Samples Co. Cis olefinic alcohols were prepared by a room temperature, low pressure catalytic hydrogenation of acetylenic alcohols in ether. A Lindlar catalyst with a trace of acetic acid was used. Some trans alcohols were prepared by reduction of acetylenic alcohols with sodium in liquid ammonia. In all syntheses ether was removed on a rotary evaporator after appropriate extractions. The crude products were purified by preparative gas phase chromatography on a 10-ft Chromosorb 102 column. Purity and identity of the samples were determined by ^1H NMR and gas phase chromatography.

0022-3654/78/2082-0940$01.00/0